Evidence for a Perturbation of Arginine-82 in the Bacteriorhodopsin Photocycle from Time-Resolved Infrared Spectra†

M. Shane Hutson,‡,§ Ulrike Alexiev,|| Sergey V. Shilov,⊥ Kevin J. Wise,⊥ and Mark S. Braiman*,⊥

Chemistry Department, Syracuse University, Syracuse, New York 13244-4100, Biophysics Program, University of Virginia Health Sciences Center, No. 456, Charlottesville, Virginia 22908, and Biophysics Group, Physics Department, Freie Universität Berlin, Arnimallee 14, D-14195, Berlin, Germany

Received February 24, 2000; Revised Manuscript Received June 26, 2000

ABSTRACT: Arginine-82 (R82) of bacteriorhodopsin (bR) has long been recognized as an important residue due to its absolute conservation in the archaeal rhodopsins and the effects of R82 mutations on the photocycle and proton release. However, the nature of interactions between R82 and other residues of the protein has remained difficult to decipher. Recent NMR studies showed that the two terminal nitrogens of R82 experience a highly perturbed asymmetric environment during the M state trapped at cryogenic temperatures [Petkova et al. (1999) *Biochemistry 38*, 1562−1572]. Although previous low-temperature FT-IR spectra of wild-type and mutant bR samples have demonstrated effects of R82 on vibrations of other amino acid side chains, no bands in these spectra were assignable to vibrations of R82 itself. We have now measured time-resolved FT-IR difference spectra of bR intermediates in the wild-type and R82A proteins, as well as in samples of the R82C mutant with and without thioethylguanidinium attached via a disulfide linkage at the unique cysteine site. Several bands in the bR → M difference spectrum are attributable to guanidino group vibrations of R82, based on their shift upon isotope substitution of the thioethylguanidinium attached to R82C and on their disappearance in the R82A spectrum. The frequencies and intensities of these IR bands support the NMR-based conclusion that there is a significant perturbation of R82 during the bR photocycle. However, the unusually low frequencies attributable to R82 guandino group vibrations in M, ∼1640 and ∼1545 cm^{-1}, would require a reexamination of a previously discarded hypothesis, namely, that the perturbation of R82 involves a change in its ionization state.

Bacteriorhodopsin (bR) is a seven-helix transmembrane protein that functions as a light-driven H^+ pump in the plasma membrane of the archaebacterium *Halobacterium salinarium* (*1*−*4*). Its three-dimensional structure has been solved to <3 Å resolution by both X-ray crystallography and electron diffraction (*1*, *5*−*14*). A retinal cofactor is covalently attached to the protein as a protonated Schiff base at Lys-216 midway through helix G, effectively dividing the protein into cytoplasmic and extracellular half-channels (*15*). Absorption of visible photons leads to an isomerization of retinal about the C_{13}−C_{14} bond from all-trans to 13-cis (*16*). In response, the protein cycles through a series of intermediates, designated K through O, as it relaxes to the initial state, accompanied by thermal reisomerization of the chromophore (*2*). The net result of this photocycle is the transport of a proton from the cytoplasm to the cell exterior (*2*−*4*).

Time-resolved and static FT-IR difference spectra have been obtained from bR photointermediates with sufficient sensitivity to detect structural changes in individual chemical groups (*17*−*19*). Such spectra have led to a description of proton-transfer events within the protein, involving the Schiff base and two critical aspartates. In unphotolyzed bR at neutral pH, the Schiff base and Asp-96 in the cytoplasmic half-channel are protonated, while Asp-85 in the extracellular half-channel is anionic (*20*, *21*). Upon the formation of the M intermediate, a proton is transferred from the Schiff base to Asp-85 (*20*). In the next step, Asp-96 donates its proton to reprotonate the Schiff base in N (*22*, *23*). Asp-96 is then reprotonated from the cytoplasm during the conversion to O (*24*).

In the wild-type protein, a proton is released into the extracellular medium concurrent with proton transfer to Asp-85 in M (*25*, *26*). The identity of the group that deprotonates in this step, the proton-release group, has been the subject of much debate. The proton-release group has been hypothesized to be either Arg-82 (*27*, *28*), Glu-204 (*30*−*34*), Glu-194 (*35*), or an H-bonded complex ion involving these groups and bound water molecules (*28*, *36*). However, evidence from site-directed mutagenesis indicates that Arg-82 itself is not the proton-release group, or at least that such a role for R82 is not obligatory, because normal H^+ release is seen in the R82Q mutant above pH 7.5 (*30*) and over a wider pH range in the double mutant R82Q/D212N (*37*).

† This work was supported by grants from the National Institutes of Health (GM-46854) and from Syracuse University. M.S.H. was supported by a predoctoral training grant (GM08323). K.J.W. was supported by NIH Grant GM34548 to R. R. Birge.

* To whom correspondence should be addressed. Phone: (315)-443-4691. Fax: (315)-443−4070. E-mail: mbraiman@syr.edu.

‡ University of Virginia Health Sciences Center.

§ Current address: Duke University Free Electron Laser Laboratory, LaSalle St. Extension, Box 90319, Durham, NC 27708.

|| Freie Universität Berlin.

⊥ Syracuse University.

10.1021/bi000426q CCC: $19.00
Published on Web 10/06/2000

The earliest high-resolution electron diffraction study of bR structure found no significant electron density for the side chain of Arg-82 (*11*). Subsequent structural models have placed the guanidino group of Arg-82 into an array of environments within the protein (*1*, *5*−*14*). In general, Arg-82 is located within a hydrophilic pocket of the extracellular half-channel at varying distances from the carboxylate groups of Asp-85, Asp-212, and Glu-204. The guanidino group points in the direction of either one or a pair of these three residues in each structural model. However, in only three of the eight structures is Arg-82 close enough to a carboxylate to form a direct hydrogen bond, in two cases to Glu-204 (*11*, *38*), and in another to Asp-212 (*7*). A more recent model has placed H_2O in this pocket with Arg-82, allowing its side chain to interact with the carboxylates indirectly through the intervening water molecules (*5*, *14*). Time-resolved electrical measurements support the hypothesis that the Arg-82 side chain moves toward the extracellular surface upon formation of the M intermediate (39).

Mutagenesis of Arg-82 has consistently been observed to have several effects on the protein, regardless of the changed residue type. First, the pK_a of Asp-85 in unphotolyzed bR is raised substantially (*27*, *30*, *40*, *42*). Thus, at neutral pH, Asp-85 is protonated, resulting in a blue chromophore instead of the wild-type purple (*41*, *42*). Only the purple protein is capable of light-driven H^+ transport (*41*). At sufficiently high pH, the purple chromophore and H^+ transport are restored in R82 mutants (*27*, *30*, *40*, *42*). However, depending upon the pH, the kinetics of H^+ release and uptake may be reversed. In this case, a proton is not released into the extracellular medium concurrent with the protonation of Asp-85 in M (*29*, *30*). Instead, the proton appears to be released directly from Asp-85 in the last, O → bR, step of the photocycle. The normal fast H^+ release, i.e., prior to H^+ uptake, occurs in wild-type bR over a large pH range, 5.8−9.5 (*30*, *43*). However, in the mutants R82K and R82Q, the limits for fast H^+ release are pH 6.5−8.0 and 7.5−8, respectively (*30*). Fast H^+ release is not restored at any pH for the mutant R82A (*42*). These experiments seem to indicate that Arg-82 itself is not the proton-release group, yet Arg-82 affects the pK_a of this group in both the bR and M states.

Recent solid-state NMR has revealed that a single arginine in bR, presumably Arg-82, gives anomalous ^{15}N resonances for the two terminal nitrogens of its guanidino group (Arg-N_η) in the M state. The splitting of the $^{15}N_\eta$ chemical shifts in M indicates a highly asymmetric environment for these two nitrogens (*44*). The NMR signals are so highly perturbed in the M state, relative to unphotolyzed bR, that there must almost necessarily be a large perturbation of the strong C−N stretch vibrations of the Arg-82 guanidino group. These vibrational perturbations should be detectable in the FT-IR difference spectrum of M and bR.

Low-temperature FT-IR difference spectra of bR and the M state phototrapped at 230 K have not previously revealed any bands directly assignable to Arg-82. Mutations of Arg-82 clearly affected difference bands from bound water molecules between 3600 and 3700 cm^{-1} (*45*). Additionally, a negative difference band near 1700 cm^{-1}, which disappeared in R82A and was greatly reduced in R82Q, was interpreted as arising from the deprotonation of Glu-204 (*45*). [However, the validity of this assignment has been questioned by recent time-resolved FT-IR spectra of Glu-204 mutants (*36*).] No bands in the low-temperature FT-IR spectra were assigned to Arg-82 itself.

Here we set out to carefully compare room temperature time-resolved FT-IR spectra of several Arg-82 mutants and wild-type bR. One advantage of time-resolved over low-temperature FT-IR spectroscopy for such comparisons is that it provides a means of more clearly delineating spectral contributions from multiple intermediates, allowing a clearer distinction of primary effects of mutation from secondary effects resulting from a perturbed photocycle. The main goals of the comparisons are, first, to identify bands assignable to Arg-82 during the bR and M states of the photocycle and, second, to interpret the FT-IR spectral perturbations in order to help unravel the role of this residue in the proton-pumping function of bR. The Arg-82 vibrational bands that we were able to identify support the prior NMR conclusion that this residue experiences a very unusual protein environment in the M state.

Additional differences between the FT-IR spectra of wild-type bR and R82A are expected to arise from structures that contribute to fast extracellular proton release, which is completely disabled in the R82A mutant (*42*). Inspection of the 1690−1800 cm^{-1} region in our spectra reveals some small differences that indicate the possible involvement of one or more carboxylic acid residues, in addition to Asp-85, in proton release. However, there is no alteration of any single band or set of difference bands carrying sufficient IR intensity to be interpretable as representing stoichiometric deprotonation of any protein residue. Our results provide preliminary data that address the question of whether Arg-82 itself undergoes partial deprotonation.

MATERIALS AND METHODS

In these experiments, wild-type bR was used in the form of purple membrane fragments isolated from the S9 strain of *H. salinarium* by previously published methods (*16*, *46*). Similar membrane fragments were prepared from the R82A and R82C mutants of bR, which were created using commercial site-directed mutagenesis kits (e.g., Quik-Change, Promega Biotech, Madison, WI) and expressed from a plasmid in the L33 strain of *H. salinarium* using previously published methods (*47*).

The R82A mutant undergoes a transition to a blue form below pH 7, i.e., with a pK_a 4−5 pH units above the same transition in the wild type (*42*). The mixture of blue and purple forms of R82A at pH 7 makes this pH unsuitable for comparisons with the wild type. However, at pH 9.5 both wild-type and R82A bR are entirely in the purple form, and their photocycle kinetics are very similar (*42*). Therefore, for time-resolved FT-IR comparisons of wild-type bR to the R82A mutant, membrane fragments were suspended in 20 mM KBr and 10 mM CAPS buffer at pH 9.5. Samples were pelleted (5000*g*), then transferred to a 2-mm-thick BaF_2 window, and partially air-dried before squeezing the sample to a thickness of ∼10 μm with a second window sealed around the edge with vacuum grease. The water content of the samples was ∼50 wt %, but the samples were kept very thin (1.5 au at 1650 cm^{-1}) since the C−N stretch bands from the guanidino group of arginine are expected to absorb maximally between 1600 and 1700 cm^{-1} (*48*), where they

overlap not only the strong ~1650 cm^{-1} H_2O band but also the multiple bands present between 1600 and 1700 cm^{-1} in FT-IR difference spectra of bR (*18*).

Isotopically Labeled ψ-Arg-82 bR. Thioethylguanidinium bromide (TEG-Br)[1] was synthesized from thiourea and 2-(bromoamino)ethane (Aldrich) by a previously published method (*49*). Through the use of [^{15}N]thiourea (Cambridge Isotope Laboratories) as a starting material, isotope labels were selectively incorporated at the two terminal nitrogens, N_η, of the TEG guanidino group.

Membrane fragments of R82C bR were labeled by suspending them in a solution of 10 mM TEG-Br in the presence of air (0.1 mL volume, protein concentration 3 mg/mL, pH 8, 10 h reaction time, unstirred) to form a disulfide linkage with the unique cysteine. The presence of TEG shifted the color of the membrane fragments from blue to purple near neutral pH, indicating that the exogenous guanidino group had substituted for Arg-82 and was successful in reducing the pK_a of Asp-85 (*41*). Previous experiments with the R82Q protein had shown that a variety of guanidino compounds could exert such an effect (*50*). Upon washing the membranes to remove any unreacted TEG, the membrane fragments remained purple, indicating that the TEG had become covalently attached to the protein. The TEG-modified side chain of Cys-82 is henceforth denoted as pseudoarginine-82 (abbreviated ψ-Arg-82) due to its ability to mimic the arginine found at this position in wild-type bR.

Reaction of R82C bR with either ^{14}N- or ^{15}N-TEG thus chemically introduced a site-specific isotope label that can report on the vibrations of the guanidino group of ψ-Arg-82. Samples of these membrane fragments between CaF_2 windows for FT-IR spectroscopy were prepared in pH 7 buffer as described previously (*51*). Wild-type bR, containing no cysteines, showed no corresponding visible absorbance change in response to similar treatment with TEG and after washing gave time-resolved FT-IR spectra that were essentially identical with untreated bR (data not shown).

Time-Resolved FT-IR Measurements. Time-resolved FT-IR data comparing the wild type and R82A mutant were collected on a Nicolet Magna-IR 860 spectrometer in step-scan mode with a 20-MHz-bandwidth photovoltaic HgCdTe detector/preamplifier equipped with both AC- and DC-coupled outputs. A pulsed, frequency-doubled Nd^+-YAG laser (532 nm, 10 mJ cm^{-2}, 3 flashes per second) was used to initiate the photocycle. Spectra were recorded with 4 cm^{-1} resolution over a bandwidth of 0−1975 cm^{-1}. An external amplifier with a gain of 25 was also applied to the transient signals to maximally utilize the ±10 V range of the internal digitizer board. A 5 μm long-pass optical filter was placed in the IR beam between the sample and detector to block scattered light from the Nd^+-YAG laser and to limit the bandwidth of the measurement, thereby averting or reducing a number of possible artifacts in time-resolved FT-IR spectra (*52*).

At each of 1088 interferogram points, the transient IR signal was digitized at 100 time points with 10 μs resolution. An entire differential interferogram was collected with the first 4160 flashes; then the interferogram collection was repeated 15−80 times for each sample. This reduced the possibility of artifacts due to irreversible photolysis of the sample within the collection time of each individual interferogram.

Limiting the time regime of the measurement to the range of 10 μs−1 ms after photolysis allowed noise rejection through the use of both high-pass (200 Hz) and low-pass (11 kHz) filters built into the spectrometer's AC-coupled analog-to-digital converter. These filters provided a means to measure the transient FT-IR spectra at a signal-to-noise ratio sufficient to characterize small changes in the highly overlapped 1600−1700 cm^{-1} spectral region. However, they prevented application of the global multiexponential fitting procedures normally used to analyze such data. The time constants associated with the low- and high-pass filters were approximately 15 and 800 μs. Thus, no time region could be selected in which the observed kinetics would be free from the influence of these filters.

The AC-coupled difference interferograms that were collected as described above were Fourier transformed using Nicolet Omnic software. Phase correction was performed using phases obtained from a DC-coupled step-scan interferogram that was collected contemporaneously with the AC-coupled time-resolved data.

Time-resolved FT-IR spectra comparing ^{14}N- and ^{15}N-ψ-Arg-82 bR, as well as a sample of wild-type bR, were collected in two separate data sets. One was measured as described above. These results confirmed the earlier collected data set, which had been obtained from independently prepared samples at lower spectral resolution but covering a longer time range. The earlier data set was obtained by using a Bruker Instruments IFS-66 FT-IR spectrometer in time-resolved step scan mode at 16 cm^{-1} resolution with a Kolmar photovoltaic HgCdTe detector (Model KMPV11-1-LJ2/239). The low- and high-pass electronic filters on this spectrometer were 200 kHz and 50 Hz, respectively. The transient signals were digitized with 10 μs resolution from 0 to 2.5 ms after photolysis. Fourier transformation was accomplished with Bruker OPUS software, and phase correction was done using doubled-angle phase correction methods described previously (*53*).

Kinetic and Spectral Analysis. Most mathematical manipulations of the time-resolved FT-IR intensity spectra were performed using Omnic (Nicolet), Opus (Bruker), or GRAMS-32 software (Galactic Industries, Salem, NH). This included band fitting, principal components analysis (PCA), and subsequent conversion of spectral intensity changes to absorbance differences.

RESULTS

Comparison of Room Temperature Photoproduct Difference Spectra of Wild-Type bR and the R82A Mutant. Typical time-resolved FT-IR difference spectra for both wild-type and R82A bR at pH 9.5, averaged over the time range 100−300 μs after photolysis, are shown in Figure 1A,B. In general, the wild-type and mutant spectra match one another remarkably well from 1000 to 1800 cm^{-1}, in accord with previous light−dark static difference spectra measured at 230 K (*45*). The negative fingerprint C−C stretch bands at 1167, 1200, and 1253 cm^{-1} and the negative ethylenic C═C stretch at 1527 cm^{-1} are unaltered in the mutant, indicating that the

[1] Abbreviations: TEG, thioethylguanidinium; PCA, principal components analysis.

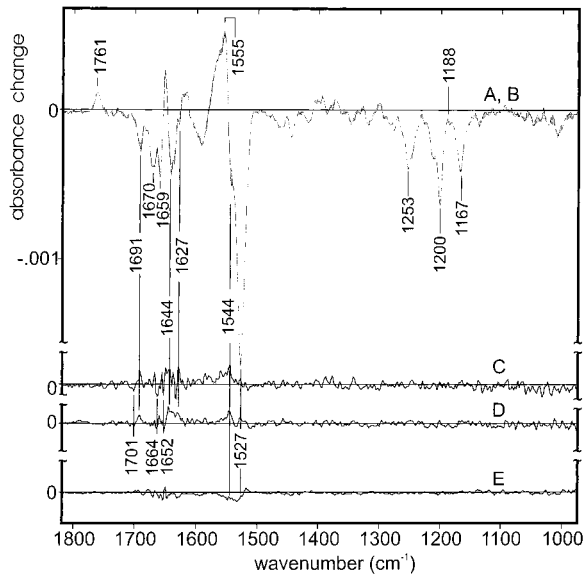

FIGURE 1: Time-resolved room temperature FT-IR difference spectra of samples of the R82A mutant of bR (A) and of the wild type (B), averaged over the time range of 100−300 μs after photolysis. To bring out the smallness of the differences between them, the area between the two spectra is shaded. (A) is the solid line bordering one edge of the shaded area; (B) is the other edge, shown without a line. The *y*-axis units are approximate values; the spectra have been scaled to match each other in size. In the wild-type spectrum (B), the ΔA band minimum at 1527 cm^{-1} reached −0.0015 absorbance unit; in R82A (A), it was −0.0037. In **(**C), the difference spectrum corresponding to (B) minus (A), i.e., $\Delta\Delta A$, is presented with the same vertical scale, except for a displaced zero indicated by the horizontal line. Spectrum D shows the average of $\Delta\Delta A$ spectra from three independently measured sample sets. One $\Delta\Delta A$ spectrum was (C), while the others were obtained similarly from two other samples each of the wild type and the R82A mutant, always rescaled to match the vertical scale of spectrum B. The combined signal averaging for the three wild-type samples combined was 157 photolysis flashes per interferogram point, and for the 3 R82A samples, it was 76 flashes per interferogram point. In (E) a control $\Delta\Delta A$ spectrum is provided showing noise and baseline reproducibility in these data sets. It was calculated by averaging $\Delta\Delta A$ spectra of two pairs of matched samples [the wild-type spectrum shown in **(**B) minus one of the other wild-type spectra used in the calculation of (D), and the R82A spectrum shown in (A) minus one of the other R82A spectra). After taking the arithmetic mean of these two $\Delta\Delta A$ spectra, the result was further divided by $(1.5)^{1/2}$ before being displayed on the same *y*-axis scale as the other spectra. This compensated for the fact that only about two-thirds as many digitizations were used to calculate the double-difference spectrum in (E), as compared to the spectrum in (D).

chromophore undergoes a normal all-trans to 13-cis isomerization upon excitation. There is no discernible negative ethylenic stretch band at 1535 cm^{-1}, nor a negative band near 1185 cm^{-1} that would indicate large contributions from a photocycle starting with 13-cis retinal in either spectrum (*54*).

Several features of the spectra show that the dominant photointermediate present over this time range is M. The positive band due to the carbonyl stretch vibration of Asp-85 COOH is at 1761 cm^{-1} as in M and shows evidence only of a small shoulder around 1754 cm^{-1} (unlabeled in Figure 1), where this vibration is known to shift in the N intermediate (*51*). The pair of negative bands at 1670 and 1659 cm^{-1} in the spectra of Figure 1A,B are of nearly equal intensity. In M, the 1659 cm^{-1} band is generally slightly larger, while in N, the 1670 cm^{-1} band is much larger (*51*). In addition, the 1188 cm^{-1} positive band due to the C−C stretch of the M and N intermediates reaches a maximum value that remains slightly below the baseline. This indicates a photointermediate mixture in these time-averaged spectra that favors M over N (*55*).

The small differences seen between the wild-type and R82A mutant time-averaged spectra in Figure 1A,B confirm those seen in the corresponding static spectra measured at 250 K (*45*). Perhaps the most obvious difference is the appearance of a resolved negative peak at 1544 cm^{-1} in the mutant (Figure 1A) that is not present in the wild type (Figure 1B). This and other smaller features can be examined more clearly by calculation of a double-difference spectrum ($\Delta\Delta A$), that is, by subtracting the scaled R82A mutant difference spectrum from the wild-type difference spectrum, as shown in Figure 1C. The scaling factor was chosen to minimize the integral of $(\Delta\Delta A)^2$ over the 1000−2000 cm^{-1} spectral range. The reproducibility of the labeled features in this double-difference spectrum, e.g., the positive band at 1544 cm^{-1}, is demonstrated by their persistence after data averaging from multiple independently prepared samples (Figure 1D). Several of the labeled features in our double-difference spectrum—most notably the 1544 cm^{-1} band—can also be discerned even from a visual comparison of 230 K static bR → M difference spectra of the wild type and the R82A mutant (*45*).

The labeled peaks in the averaged wild-type/R82A double-difference spectrum (Figure 1D) are above the noise levels in a control double-difference spectrum (Figure 1E). The largest baseline errors in this control double-difference spectrum, lying right under the 1527 cm^{-1} ethylenic band, are nearly as large as the labeled features in the averaged wild-type/R82A double-difference spectrum (Figure 1C,D). These baseline errors are distinct from spectrometer noise, which is expected to be highest in regions of strong background absorbance, e.g., the region near 1650 cm^{-1}, where the overall transmittance of the sample was typically 2−3% as a result of water and amide I absorption bands (absolute absorbance spectra not shown). Transmittance in the amide II region typically reached a minimum of 10−15% near 1550 cm^{-1}, and this strongly absorbed spectral region was narrow enough that it cannot reasonably explain the large features in the 1510−1530 cm^{-1} range in the control difference spectrum (Figure 1E). Instead, it is likely that these baseline deviations arise from the presence of small amounts of photocycle contaminants produced by nonlinear effects (e.g., two-photon events), which are not perfectly matched in various samples. The size and even the sign of the large baseline deviations between 1510 and 1535 cm^{-1} in the control spectrum (Figure 1E) are not at all reproducible in different samples, in contrast to the 1544 cm^{-1} band in Figure 1C,D.

The bands in the wild-type/R82A double-difference spectrum (Figure 1C) are generally small and unreproducible (below the noise level), except in two distinct regions. First, there is a positive double-difference band centered at 1544 cm^{-1}. This band is quite large in integrated intensity, 0.35 ± 0.05 times the size of the 1761 cm^{-1} COOH carbonyl band due to Asp-85 in Figure 1A,B, as determined by fitting the ±20 cm^{-1} region around each band to a single Gaussian peak and a linear baseline. The magnitude of the 1544 cm^{-1} difference band is masked in a visual inspection of the raw

(single-difference) time-resolved FT-IR spectra (Figure 1A,B), due to the large overlapping bands at (−)1527 and (+)1555 cm^{-1}. The assignment of the 1544 cm^{-1} band is not immediately obvious, since arginine does not generally exhibit any strong IR absorption in the 1500−1600 cm^{-1} range. It would be tempting to attribute this strongest double-difference band to a chromophore baseline artifact. This is unlikely, however, because unlike the baseline deviations between 1510 and 1530 cm^{-1} in the control spectrum (Figure 1E), the 1544 cm^{-1} double-difference band is reproducible in sign and (to within a factor of 1.5) in relative magnitude in multiple independent sample pairs that are carefully matched in thickness and water content. A possible alternative assignment of the 1544 cm^{-1} band would be to an amide II vibration of a group that is perturbed by the R82A mutation. Only the site-directed isotope labeling experiments (see below) indicate that the latter interpretation is probably wrong and that the 1544 cm^{-1} band in the double-difference spectrum (Figure 1C) is likely due to a vibration of Arg-82 itself.

The second region with sizable double-difference bands lies between 1620 and 1700 cm^{-1}. Again, it is evident in the raw time-resolved spectra of Figure 1A,B that the mutation has induced some spectral perturbations in this region, but it is possible to identify specific peaks only in the double-difference spectrum (Figure 1C,D). There are three positive bands that peak near 1627, 1644, and 1691 cm^{-1}, and three negative bands at 1652, 1664, and 1701 cm^{-1}. Substituted guanidinium compounds have two asymmetric C−N stretch vibrations with considerable infrared intensity between 1600 and 1700 cm^{-1} (*48*, *56*−*58*). Thus some, but probably not all, of the bands in the 1600−1700 cm^{-1} spectral range could be due to vibrations of Arg-82.

Time Dependence of Photointermediate Compositions in the Wild Type and the R82A Mutant. Comparisons of the wild-type and R82A mutant spectra are complicated by the possibility of different mixtures of intermediates resulting from differences in the kinetic behavior of the samples. In addition to the M state of bR, both the L and N states are expected to be present in significant amounts between 10 μs and 1 ms. There are substantial changes in the IR spectra of L, M, and N, especially in the 1600−1700 cm^{-1} range (*18*). Secondary effects due to different photointermediate compositions could therefore produce spectral changes in the R82A mutant as big as the primary changes expected due to the elimination of arginine spectral bands.

The possibility of different photointermediate compositions is a problem for comparing spectra obtained either in a steady state mixture at low temperature (*45*) or in the time-evolving mixture at room temperature. In the latter case, however, careful measurement of the spectral time dependence can help to distinguish between effects of the mutation on relative photointermediate compositions and effects on the structures of individual photointermediates.

To help assess the photointermediate mixture present at various times from 10 to 950 μs, the kinetics of absorbance changes at 1188 cm^{-1} are shown in Figure 2. It is clear from these data that the photocycle kinetics are very similar over this time range for both wild-type and R82A bR. Before 70 μs, both proteins show a substantial positive band at 1188 cm^{-1} indicative of an L intermediate. The absorbance change at 1188 cm^{-1} then retreats to below the baseline from 100 to 700 μs as a result of the chromophore deprotonation in M. Only after ∼750 μs do the signals become positive again, marking the transition to the N intermediate and reprotonation of the retinylidence Schiff base chromophore (*55*). The data shown here indicate that, over the time range included in the average of Figure 1 (100−300 μs), the predominant intermediate is M and that the relative concentrations of other minor photointermediates are well matched in the wild type and R82A mutant. Therefore, the largest spectral differences between the wild type and the R82A mutant in Figure 1 cannot likely be attributed to altered relative concentrations of different photointermediates.

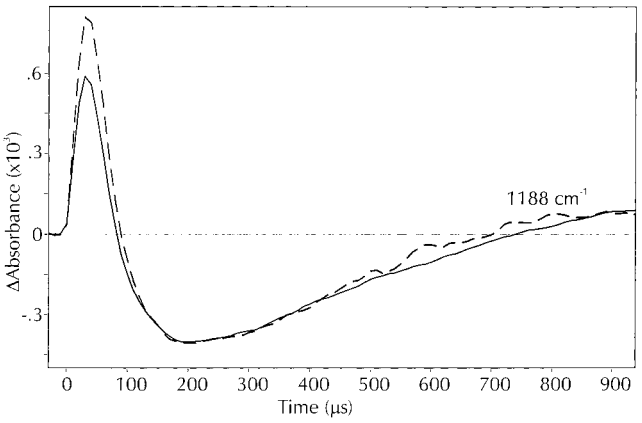

FIGURE 2: Absorbance changes as a function of time after photoexcitation at 1188 cm^{-1} for wild-type (solid line) and R82A (dashed line) bR. The vertical axis represents the absorbance change for the wild-type sample. The curve for the R82A mutant was rescaled to reach the same minimum value near 200 μs.

Based on the observation of similar kinetics in the wild type and R82A mutant, it makes sense to calculate the time-dependent double-difference spectrum with somewhat faster time resolution than in Figure 1. The resulting time-dependent double-difference spectra in Figure 3 help to confirm that the labeled features in the double-difference spectrum of Figure 1 can reliably be assigned to the M intermediate state. The data of Figure 3 also demonstrate what happens to those features as the N intermediate is formed. The flatness of the baseline in these double-difference spectra, especially the absence of any significant features in the 1150−1200 cm^{-1} range, is a very clear demonstration that the time evolution of features, such as the clear growing-in of the positive 1558 cm^{-1} band, cannot be attributed to different amounts of N forming in the wild type and mutant, even though N is well-known to have a strong IR absorption near 1555 cm^{-1}. Instead, the 1558 cm^{-1} band appears to signal a distinct structural difference between the N states of the wild type and R82A mutant.

Continuum Absorbance Changes in R82A bR. Continuum absorbances are due to protons in highly polarizable double-well potentials that lead to absorbance over a broad spectral range in the mid-IR (*59*). Since FT-IR difference spectra of the bR photocycle are free of specific bands above 1800 cm^{-1}, the continuum absorbance changes in R82A can be followed by the average absorbance change between 1800 and 1900 cm^{-1} as a function of time. These changes are shown in Figure 5, alongside similar measurements for wild-type bR. The magnitude of these changes is only ∼2% of the negative 1527 cm^{-1} ethlyenic C═C stretch band.

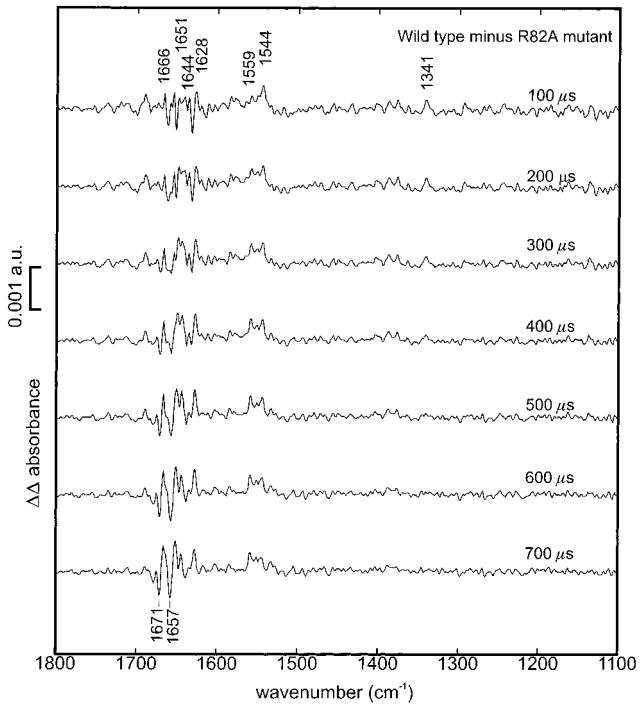

FIGURE 3: Temporal evolution of the double-difference spectra ($\Delta\Delta A$) between the wild-type and R82A samples. The same scaling factor as in Figure 1C was used for all time points. Each time point represents the average of 10 individual 10 μs slices centered around the indicated time.

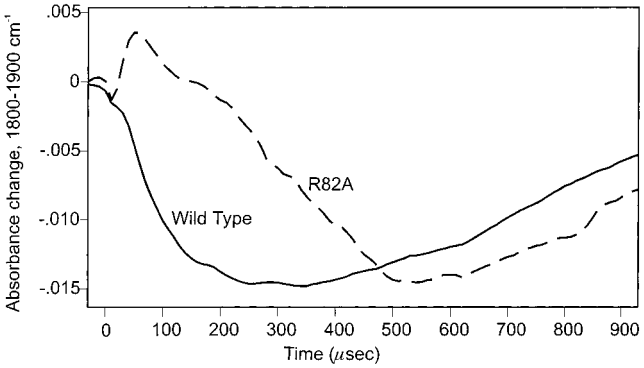

FIGURE 4: Continuum absorbance change ΔA as a function of time after photolysis for wild-type (solid line) and R82A (dashed line) bR. The continuum ΔA was calculated as the average ΔA over the range 1800−1900 cm^{-1}, relative to the magnitude of the absorbance change at 1527 cm^{-1}.

Substantial differences exist in these absorbance changes between R82A and wild-type bR during the first 400 μs after the flash. While both reach similar levels by 650 μs, the time course of this change is delayed in the R82A mutant. On the basis of the data in Figures 2 and 3, the wild-type and R82A photocycles are both dominated by an M intermediate between 100 and 700 μs. Thus, there are continuum absorbance changes in the M state of wild-type bR that do not appear in the M state of R82A. However, Figure 4 shows that once the N photointermediate arises, the continuum absorbance changes are the same in the wild type and mutant.

Time-Resolved IR Spectra of ψ-Arg-82 bR. To help to assign vibrational frequencies of Arg-82 in bR and its photoproducts, the mutant R82C was chemically labeled with either $^{14}N_\eta$- or $^{15}N_\eta$-TEG. The resultant pseudoarginine (ψ-Arg) side chain at position 82 was capable of substituting

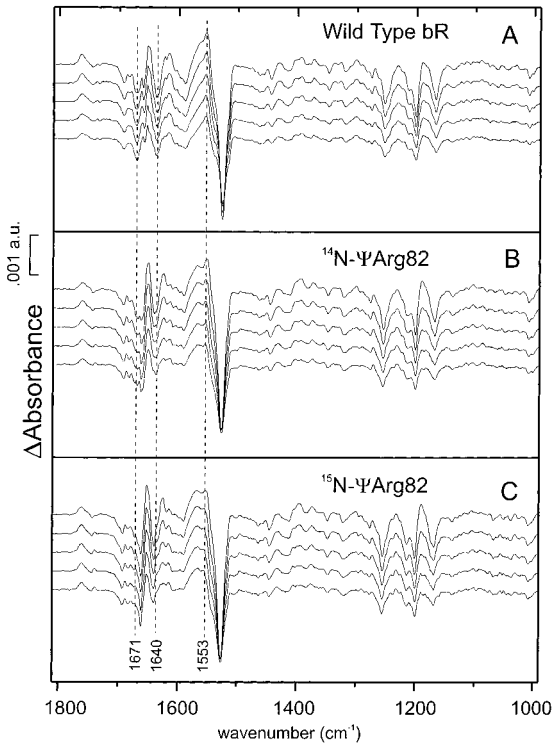

FIGURE 5: Time-resolved FT-IR difference spectra of (A) wild-type, (B) ^{14}N-ψ-Arg-82, and (C) ^{15}N-ψ-Arg-82 bR. The series of spectra in each panel represents the evolution of the spectrum at five different time ranges centered about 140, 280, 420, 560, and 700 μs after photolysis, increasing in delay time from top to bottom. Each plotted difference spectrum is the average of 14 individual time slices measured with 10 μs temporal resolution. The ΔA scales of all panels are identical.

for the wild-type arginine as evidenced by a blue shift of the λ_{max} of R82C bR back to 565 nm upon reaction with TEG and subsequent washing with pH 7 buffer. Unlike the similarly sized blue shift that occurred with ethylguandinium or guanidinium itself, the blue shift with TEG was stable under repeated washings (data not shown), indicating irreversible formation of a stable disulfide linkage between TEG and the protein. That is, creation of ψ-Arg-82 largely reversed the pK_a upshift of Asp-85 in the purple-to-blue transition of the R82C mutant. The pK_a of this transition for wild-type bR is 2.6, that for the R82C mutant is 7.4, and that for the ψ-Arg-82 bR is 3.7. In addition, the ψ-Arg-82 bR exhibited a wild-type-like fast proton-release phase at pH 7 (data not shown).

Time-resolved FT-IR spectra of the ψ-Arg-82 bR sample were measured. Series of these spectra, averaged to an effective time resolution of 150 μs, are shown in panels A−C of Figure 5, respectively, for wild-type bR and for the ^{14}N-ψ-Arg-82 bR and ^{15}N-ψ-Arg-82 bR samples. The $^{14}N \rightarrow {}^{15}N$ isotope substitution is expected to cause 5−10 cm^{-1} downshifts in two C−N stretch vibrations, normally expected in the range of 1600−1700 cm^{-1} for the protonated guanidino group of arginine (*56*).

There is a clear signal for such a downshift in the negative 1671 cm^{-1} band in ^{14}N-ψ-Arg-82 bR (Figure 5B). The downshifted frequency is in a congested spectral area of poorer signal-to-noise ratio, due to the presence of strong background absorption due to water and amide I vibrations. However, there is evidence that this band has downshifted to near ~1664 cm^{-1} in ^{15}N-ψ-Arg-82 bR, since a similarly

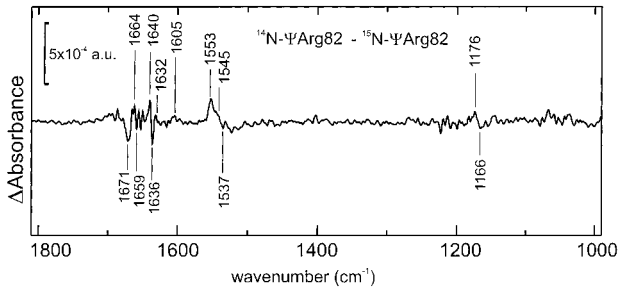

FIGURE 6: Double-difference FT-IR spectrum of ^{14}N-ψ-Arg-82−^{15}N-ψ-Arg-82 bR, calculated from the average time-resolved spectra (220−360 μs) corresponding to the bR → M transition. In carrying out the subtraction, the ^{15}N-ψ-Arg-82 spectrum was rescaled relative to the ^{14}N-ψ-Arg-82 spectrum in order to minimize the bands in the double-difference spectrum below 1500 cm^{-1}.

sized positive band appears in this spectral region in the double-difference spectrum (Figure 6).

The poor signal-to-noise ratio in the 1630−1660 cm^{-1} range makes it difficult to say whether there are any vibrations in this range, either in the bR or in the M state, that downshift appropriately with ^{15}N substitution to be arginine C−N stretches. The strongest candidate for such an isotope-sensitive band is a differential signal at 1640/1636 cm^{-1} in the double-difference spectrum (Figure 6). The sign of this differential feature is consistent with the predicted heavy-isotope-induced downshift only if it arises from a vibration present in the M state, i.e., a vibrational band that is positive in the single-difference spectra in Figure 5.

In addition, the strongest band with an isotope-induced downshift appears, rather unexpectedly for an arginine C−N stretch vibration, below 1600 cm^{-1} (Figures 5 and 6). A positive band at ∼1553 cm^{-1}, clearly seen in the ^{14}N$_\eta$-ψ-Arg-82 spectra (Figure 5B), clearly decreases in intensity in the ^{15}N$_\eta$-ψ-Arg-82 spectra. The downshifted frequency is near 1535 cm^{-1}, but overlapping bands in this region of the time-resolved spectra are too large to see this shift without the aid of a double-difference spectrum (Figure 6). In this double-difference spectrum, the negative 1535 cm^{-1} band appears somewhat weaker than the positive 1553 cm^{-1} band. Thus isotope labeling generally supports assignment of bands near 1640 and 1550 cm^{-1} to C−N stretch vibrations of ψ-Arg-82 in the M state, but a significant intensity decrease of the latter band may also accompany its isotope-induced downshift.

Comparison of the ψ-Arg-82 bR spectra with those of the wild type subjected to similar treatment (Figure 5A) reveals that the photocycle kinetics are similar in the first 500 μs (i.e., the L → M transition) but altered in the later portion of the time range examined (the M → N transition). The wild-type protein undergoes a transition from M to N between 500 and 2500 μs (only a portion of this time range is shown in Figure 5), as evidenced by a shift of the Asp-85 COOH carbonyl stretch band from 1761 to 1754 cm^{-1} (*51*). In both ψ-Arg-82 samples, however, this band remains at 1758 cm^{-1} throughout the time range to 2500 μs (data not shown), indicating the invariant presence of a perturbed M state throughout this time range. In addition, there is a change in the appearance of a positive peak at 1557 cm^{-1}, which appears in the late M and N intermediates of wild-type bR and has been attributed to an amide II vibrational mode indicative of a protein conformational change (*51*). We observe this band in spectra of the wild-type bR (Figures 5A and 1A) and also in the R82A mutant at pH 9.5 (Figure 1B), but it has changed shape in the spectra of both isotopic variants of ψ-Arg-82 bR at pH 7. Corresponding with this change in amide II band shape, it is also evident from the UV/visible photocycle measurements (data not shown) that the ψ-Arg-82 bR has an altered equilibrium mixture between M, N, and O intermediates in time ranges above 1 ms, relative to wild-type bR. Thus one must be somewhat cautious when extrapolating assignments in the difference spectra of ψ-Arg-82 bR to the wild type. We therefore concentrate on the first part of the time range, where proton release takes place and where photoproduct compositions as detected by the UV/visible measurements (not shown) are similar to the wild type.

The extreme care that was taken to match the conditions for labeling the R82C samples with the two different isotope variants of TEG leads to great confidence that there is a strong C−N stretch vibration of Arg-82 somewhere in the vicinity of 1550 cm^{-1} in these samples. The presence of a strong positive band of similar frequency in double-difference spectra of the wild type and R82A (Figure 1) indicates that this is the single best candidate for a perturbed Arg-82 C−N stretch vibration in the M state. The integrated intensities of the positive bands near 1545−1550 cm^{-1} in Figures 1 and 6 are similar, corresponding to 30−40% of the integrated intensity of the 1760 cm^{-1} band due to Asp-85.

DISCUSSION

Our measurements of time-resolved FT-IR spectra of Arg-82 mutants of bR were motivated by two previous observations. First, solid-state NMR experiments have revealed an unusual 24 ppm splitting of the ^{15}N$_\eta$ resonances for a single arginine residue in the M state but only unperturbed chemical shift values for this arginine in unphotolyzed bR (*44*). This indicates an unusually asymmetric environment for the two terminal nitrogens of some arginine in M, most likely Arg-82 because this is the only arginine in the active site of the protein and, therefore, the only one likely to undergo such a large perturbation.

A structural perturbation sufficient to produce the unusual arginine NMR signal should also affect the C−N stretch vibrational bands of the same residue, resulting in substantial bands assignable to guanidino group vibrations in FT-IR difference spectra of the bR → M reaction of the wild-type protein. Despite prior comparisons of bR → M difference spectra of wild type and Arg-82 mutants of bR (*45*), no such bands have previously been assignable. However, this is largely because the previously published Arg-82 mutant spectra were all steady-state photoproduct difference spectra obtained at 230 K. The likely presence of altered steady-state photoproduct mixtures in the mutants meant that observed spectral differences could not be unambiguously assigned to Arg-82 vibrations. Measurement of time-resolved FT-IR spectra at physiological temperatures, as well as measurement of spectral shifts in site-directed isotope-labeled samples, allows resolution of these ambiguities.

A second previous observation motivating our experiments on R82 mutants is that H^+ release to the extracellular medium in M is abolished in the R82A mutant (*42*). It is therefore expected that FT-IR difference bands from the proton-release

group should be present in the bR → M difference spectrum of the wild-type protein but absent in that of the R82A mutant. A careful comparison of these difference spectra is therefore expected to reveal vibrational difference bands that can reasonably be interpreted as arising from the deprotonation of an ionizable residue.

Surprisingly, the two sets of bands we were looking for overlapped. That is, the strongest IR bands assignable to Arg-82 in the bR and M states are also reasonable candidates for bands that signal proton release, i.e., Arg-82 deprotonation. However, because an arginine deprotonation has never been directly observed to occur inside a protein under physiological conditions and because there are reasonable alternative explanations, the data presented herein do not yet support an unequivocal conclusion about a direct role for Arg-82 in proton release.

Assignment of Bands to Arginine C−N Stretches of Arg-82. The most prominent difference between the bR → M spectra of the wild type and R82A, which shows up as a dip in the latter spectrum with a minimum near 1545 cm^{-1} (see Figure 1), appears at first glance to be due to a vibration present in the bR state of the mutant that is not present in the wild type. Alternatively, it could be due to a positive band present in the M state of the wild type but not the R82A mutant, which happens to cancel out a negative band present at almost exactly the same frequency in the bR state of both the wild type and mutant. The former explanation could only be the case if the discrepancy between the wild type and mutant is due to a secondary effect, since there is no vibration due to an alanine side chain that would be expected to occur near 1544 cm^{-1}. Additional differences between R82A and the wild type are less visible in the raw difference spectra (Figure 1A,B) but are revealed by calculation of the double-difference spectrum (Figure 1C,D) to be nearly as large as the difference at 1544 cm^{-1}.

The first potential concern about assignment of these bands to arginine-82 vibrations is whether they may arise due to differences in photointermediate composition. We have made the measurements at a pH where these differences between wild type and R82A are known to be minimized. Furthermore, the temporal correlations of the bands that we attribute here to arginine-82 vibrations in the M state are distinct from those that typically occur in the known bR photointermediates. For example, the 1544 cm^{-1} positive band in Figure 1C,D clearly shows a decay in Figure 3 during the known time scale of the M → N transition. This would tend to indicate that this band might arise from the presence of different relative amounts of M and N in the wild-type and mutant samples but almost certainly not as a result of different amounts of K or L, for example, for which this band's kinetic behavior in Figure 3 is much too slow. However, this frequency, 1544 cm^{-1}, has never previously been observed as a prominent peak in M or N difference spectra (*22*, *23*). If there were different relative amounts of M and N present on these time scales, we would expect to see much more pronounced double-difference bands at frequencies of known M/N difference features, e.g., 1188 and 1755 cm^{-1}, where only relatively small $\Delta\Delta A$ signals are seen (Figure 3). A more detailed mathematical analysis of the data shown in Figures 1 and 3, based on principal components analysis (PCA) and published elsewhere (*63*), confirms that the major spectral differences we observe between wild-type and R82A samples cannot be associated with any of the photointermediates already present in the wild-type sample.

The labeled features in the double-difference spectra of Figure 1C,D cannot therefore easily be explained simply by altered compositions of known photoproducts. At this time we cannot rule out completely that these features may be due to unknown photointermediate(s) that constitute(s) a minor component (<5%) in the wild-type photocycle, which may have a greater or smaller presence in the R82A photocycle. Nevertheless, the similar time constants for the major photocycle events (Figure 2) and the overall time evolution that we have measured for the double-difference features (Figure 3) lend confidence to our conclusion that these features do not likely arise from different compositions of the known major photoproducts or from introduction into the photocycles of large fractions (>5%) of new photoproducts in the mutant. Drawing such a conclusion from time-resolved spectroscopy is much easier than for static low-temperature FT-IR difference spectroscopy, in which photostationary-state compositions are generally more difficult to analyze and where there is added concern about the possibility of new two-photon reactions from the mutant's photointermediates. In the latter case, there is no clear way to control for the possibility of rather large secondary effects due to altered photoproduct compositions in a mutant. Only with time-resolved FT-IR difference spectroscopy, where the time evolution of the photointermediate mixture is obtained, can the possibility of altered photointermediate compositions in the wild-type and R82A samples be reduced from a major to a minor uncertainty.

Assignment of bands to Arg-82 based on changes between the wild-type and R82A bR → M spectra are complicated by at least two additional secondary effects of R82 mutations. First, normal H^+ release, i.e., H^+ release concurrent with the rise of M, does not occur in R82A (*42*). As discussed below, there is evidence that the H^+ release involves multiple chemical groups within the protein. Therefore, IR bands that change between wild type and the mutant could correspond to vibrations of the proton-release group(s) rather than of Arg-82. Second, there is NMR evidence that light-induced backbone conformational changes linked to the transient protonation of Asp-85 do not occur when Arg-82 has been mutated (*60*). Therefore, IR bands that change between the wild type and mutant could be assignable to peptide backbone vibrations. Both of these secondary effects might produce difference bands in the 1500−1700 cm^{-1} spectral region where bands arising from an Arg-82 perturbation are expected. Thus, in the strictest sense, the observed double-difference bands in Figure 1C must be considered only as candidates for assignment to Arg-82.

Certainly, a conformational change present in the wild-type photocycle and absent in the R82A intermediates could give rise to amide I difference bands between 1600 and 1700 cm^{-1} and amide II difference bands between 1500 and 1600 cm^{-1}. The 2-fold increase in intensity of the 1646 and 1666 cm^{-1} double-difference bands during the M → N transition (Figure 3) may indicate contributions from the large conformational changes present in this transition (*51*). Since the double-difference band at 1544 cm^{-1} instead decays during this transition (Figure 3), it is less likely that amide II modes contribute to it.

Another potential concern is that the double-difference band at 1544 cm^{-1} (Figures 1 and 3) could arise from an ethylenic C═C stretch of the retinylidene chromphore. Raman spectra of the R82Q mutant at pH 5 indicated that it contained a 1:1 mixture of all-trans:13-cis retinal even in the light-adapted state (*54*). The main ethylenic band of the 13-cis component of dark-adapted, wild-type bR is at 1536 cm^{-1} (*61*). Any positive band in the double-difference spectrum might be due to a negative band present in the R82A spectrum that is absent in the wild type. Therefore, if a significant fraction of unphotolyzed R82A bR contained a 13-cis chromophore, infrared absorption from this component might conceivably give rise to a positive double-difference band near 1536 cm^{-1}. However, this is not the best explanation for the band observed in Figure 1 at the considerably higher frequency of 1544 cm^{-1}. The expected kinetics for a 13-cis photocycle contaminant also do not match those observed for the 1544 cm^{-1} double-difference band, which clearly decays during the M → N transition (Figure 3). The photocycle of the 13-cis component of dark-adapted bR decays back to the original state with a time constant of ∼30 ms, much slower than the ∼600 μs decay time observed for the double-difference band at 1544 cm^{-1} (kinetic fits not shown here; see also ref *62*).

We have attempted to address concerns about secondary effects of the R82A mutation by obtaining time-resolved FT-IR spectra of site-specific isotope-labeled ψ-Arg-82 bR. Double-difference spectra of $^{14}N_{\eta}$- minus $^{15}N_{\eta}$-ψ-Arg-82 bR reveal a shift of a positive band from ∼1550 to 1535 cm^{-1} upon ^{15}N substitution of the guanidino group of ψ-Arg-82 (Figures 5 and 6). In addition, there is a downshift of a positive band from 1640 to 1636 cm^{-1}. The positive bands at 1544 and 1644 cm^{-1} in wild-type but not R82A bR (Figure 1D) might correspond to the isotope-sensitive bands near 1553 and 1640 cm^{-1} in the ψ-Arg-82 bR spectrum (Figures 6 and 7); the small frequency differences could easily arise from the slightly different side-chain position of Arg-82 and ψ-Arg-82.

However, comparison of the ψ-Arg-82 bR spectra (Figure 5B,C) with those of the wild type (Figure 5A) indicates additionally that the overall photocycle is somewhat perturbed in the TEG-labeled mutant. While pseudoarginine is able of mimic the effect of Arg-82 on the pK_a of Asp-85 in unphotolyzed bR (*41*), the replacement of a C−C bond in arginine with the C−S−S−C bridge of pseudoarginine is sufficiently nonconservative so as to hamper the full restoration of a wild-type photocycle. Some degree of caution is therefore warranted in extrapolating the results from ψ-Arg-82 to wild-type bR, at least in the last part of the photocycle.

Assignment of vibrational frequencies to Arg-82 must also take into consideration the known frequencies and IR intensities of the guanidino group, based on spectroscopy of model compounds. The strongest infrared bands of the arginine side chain below 1800 cm^{-1} are due to asymmetric C−N stretches of the guanidino group (*56*). For aqueous arginine, these bands are located at 1633 ± 3 and 1673 ± 3 cm^{-1}, with peak extinction coefficients of 300 ± 20 and 420 ± 40 M^{-1} cm^{-1}, respectively (*48*). In the same work, by comparison, the peak extinction coefficient of a protonated aspartic acid carbonyl stretch was found to be 280 ± 20 M^{-1} cm^{-1}. Thus, a major perturbation of an arginine would be expected to result in FT-IR difference bands in the 1600−1700 cm^{-1} region that are comparable in size to the 1761 cm^{-1} COOH band of Asp-85 (*20*). The most important result of the wild-type/R82A comparisons in Figures 1 and 3 is therefore not that they indicate arginine-82 in the M state may have C−N stretch vibrations at 1544, 1628, 1640, or 1690 cm^{-1}. It is rather that other possible frequencies for perturbed arginine-82 vibrations in the M state are strongly excluded, since such vibrations would be expected to be observable above the very flat baseline and very unlikely to be canceled out by secondary effects of the mutation.

It is nevertheless important to consider whether any of the reproducible differences between the wild-type and R82A spectra (Figure 1) could be due to vibrations of Arg-82. These include three positive bands at 1627, 1644, and 1666 cm^{-1}, and two negative bands near 1657 and 1671 cm^{-1}, that increase in size as N accumulates (Figure 3). The other strong bands in the double-difference spectra of wild-type and R82A bR are a positive band at 1544 cm^{-1} and a negative band at 1632 cm^{-1} (Figures 1 and 3). These bands due to the bR state are present in the bR → M difference spectrum and appear to decay as M is converted to N (Figure 3). It seems likely that at least some of these bands are due to amide I vibrations that are perturbed by the R82A mutation. However, there is a negative band near 1671 cm^{-1}, associated with the bR state in the $^{14}N_{\eta}$-ψ-Arg-82 spectra (Figure 5B), that clearly undergoes an isotope-induced downshift (Figures 5C and 6), indicating that it probably corresponds to an Arg-82 guanidino group C−N stretch. This is a very normal frequency for such a vibration, and this assignment supports the prior conclusion that Arg-82 in the bR state is in a typical hydrogen-bonded environment (*44*).

Assignment of bands at ∼1544 and ∼1644 cm^{-1} in the M state of wild-type bR to arginine side-chain vibrations is also supported by their behavior in the R82A mutant (Figures 1 and 3) and by observed downshifts of bands near these regions (1553 and 1640 cm^{-1}) upon $^{14}N/^{15}N$ substitution in the ψ-Arg-82 bR samples (Figures 5 and 6). The availability of samples that differ by only ^{15}N substitution at two atoms in the entire 26-kDa protein (Figures 5B,C and 6) provides an important test for vibrational assignments. In this case, observed downshifts between the two chemically identical samples are very unlikely to be due to secondary effects arising from different protein conformations.

However, these assignments are outside the expected ranges of C−N stretches of arginine and are therefore likely to be controversial. The data do leave open the possibility of alternative assignments. If we assume that the observed effects of Arg-82 mutational and isotopic substitution on ∼1545 and ∼1640 cm^{-1} IR bands are due to an unlucky combination of artifacts, then it is still possible to make a more conservative assignment of Arg-82 C−N stretch vibrations in the range in which protonated guanidino groups generally absorb strongly, i.e., 1600−1700 cm^{-1}. In this case, both of the two positive bands in the double-difference spectrum near 1644 and 1627 cm^{-1}, as well as the negative bands near 1664 and 1652 cm^{-1} (Figure 1), are assigned to Arg-82. The size of these bands relative to the Asp-85 COOH stretch band at 1761 cm^{-1} would indicate that there is a significant perturbation of the Arg-82 environment at this point in the photocycle. When the N photointermediate begins to accumulate at later times, these difference bands become even larger (Figure 3).

Structural Interpretation of Arg-82 Vibrational Frequencies. If the assignments of bands at ~1670 cm^{-1} in the bR state and at ~1645 and ~1545 cm^{-1} in the M state of wild-type bR to arginine side-chain vibrations are correct, accounting for them structurally would probably require that the Arg-82 guanidino group deprotonate, since only deprotonated guanidine compounds have been observed to have strong vibrations with C−N stretching character in the frequency range 1500−1600 cm^{-1}. For example, spectra of ethylguanidine in 1 M sodium methoxide showed that the strongest C−N stretch vibrational bands are shifted to the region between 1500 and 1600 cm^{-1} (*56*). On the basis of the FT-IR data alone, therefore, Arg-82 deprotonation would perhaps be the most strongly supported conclusion. However, on the basis of other kinds of evidence, this assignment appears questionable. In particular, since fast proton release can be restored in the R82Q mutant of bR above pH 7.5 (*30*) and in the double mutant R82A/G231C over a wider pH range (*64*), deprotonation of Arg-82 is not required for H^+ release in M. This argues against the possibility that the Arg-82 protonation state is perturbed at this point in the photocycle.

If, instead, the alternative assignments discussed above are correct, i.e., if all of the Arg-82 C−N stretch vibrations are in the range of 1600−1700 cm^{-1} at all stages of the photocycle, then the specific environment changes that give rise to the observed shifts are not unambiguously defined by the band frequencies. However, a few possibilities are probably excludable.

Model compound studies of ethylguanidinium (EG) salts dissolved in nonpolar solvents revealed a dependence of the guanidino asymmetric C−N stretch vibrations on the nature of the counterion. For ion pairs of EG^+ and halides in $CHCl_3$/MeOH (97:3), the highest C−N stretch frequency is near 1670 cm^{-1} (*58*). For EG^+·acetate ion pairs, this frequency increases to 1684 cm^{-1} (*58*). Infrared spectra of solid films of EG^+·carbonate and EG^+·OH^- exhibit C−N stretch frequencies of 1695 and 1693 cm^{-1}, respectively (*56*). Thus, ion pairing of the positively charged guanidino group with strong oxyanions is quite generally expected to push the highest C−N stretch frequency into the region 1680−1695 cm^{-1}. In contrast, the highest Arg-82 C−N stretch frequency in both bR and M states appears to be below this range. Rather, the highest frequency assignable to an Arg-82 C−N stretch in the M state, i.e., the highest frequency positive band in the isotope-sensitive double-difference spectrum (Figure 5), is at 1664 cm^{-1}. Although we believe this positive band represents the ^{15}N-downshifted frequency of a bR (negative) band at 1671 cm^{-1}, it might alternatively correspond to an M (positive) band.

The absence of evidence in Figures 5 and 6 for arginine C−N stretch vibrations above 1670 cm^{-1} in M argues against models in which Arg-82 forms a direct ion pair with a hydroxide ion or a carboxylate to facilitate proton release in M. Instead, the lower-frequency range over which double-difference bands are observed suggests that a protonated Arg-82 would be in a less strongly hydrogen-bonded environment in both unphotolyzed bR and in the M and N intermediates, i.e., that it is H-bonded to neutral groups rather than carboxylate, phenolate, and/or hydroxide.

Infrared Bands of the Proton-Release Group of bR. Since fast H^+ release is abolished in R82A bR (*42*), the reconstructed double-difference spectra of wild-type versus R82A bR should also contain bands due to the proton-release group. The most widely supported candidates for this group, based primarily on site-directed mutagenesis studies, are probably Glu-204 and Glu-194 (*30*−*35*). As in a previous comparison of wild-type and R82A mutant difference spectra at −20 °C (*45*), we observe in the room temperature bR → M difference spectra that a small, negative band at ~1701 cm^{-1} in the wild type (Figure 1A) is missing in the R82A mutant (Figure 1B), giving rise to a negative band at this frequency in the double-difference spectrum (Figure 1C). This could indicate the possible involvement of a carboxylic acid residue in proton release. The ~1701 cm^{-1} band in wild-type bR → M difference spectra was previously assigned to the carbonyl vibration of the protonated form of Glu-204 (*45*), and this residue was furthermore assigned as the proton-release group.

However, time-resolved FT-IR spectra of the E204Q mutant have recently contradicted this assignment (*36*). Furthermore, the amplitude of the 1701 cm^{-1} double-difference band is very small compared to that of the 1761 cm^{-1} band that is present in the bR → M difference spectrum of both the wild type and R82A (Figure 1A,B). The latter band is generally recognized as corresponding to stoichiometric deprotonation of Asp-85 during the photocycle (*20*). The 5−10 times smaller amplitude at 1701 cm^{-1} suggests that it corresponds to at most a partial deprotonation. Finally, the 1701 cm^{-1} negative band is counterbalanced by a similarly sized positive double-difference band at 1691 cm^{-1} (Figure 1C), suggesting that both members of this pair might alternatively be due to a perturbation, rather than a partial deprotonation, of a COOH group.

The positive band at ~1545 cm^{-1} is in a frequency range that could correspond to the asymmetric COO^- stretch of glutamate residues (*48*). However, if this signal were to represent the deprotonation of a glutamic acid residue, then an additional positive band corresponding to the symmetric COO^- stretch should be observed near 1400 cm^{-1} with ~60% relative intensity (*48*), compared to the positive band at 1544 cm^{-1}. A negative band from the COOH stretches above 1700 cm^{-1} should also be observed with ~40% relative intensity (*48*). As none of these are present in the double-difference spectra (Figure 3), the band at 1544 cm^{-1} does not likely represent the deprotonation of a glutamic acid residue.

Besides bands near 1700 cm^{-1}, there are others in the wild-type/R82A double-difference spectrum (Figure 1C) that can be hypothesized to represent protonation changes of the proton-release group. However, few of them correspond to characteristic frequencies of ionizable groups present in bR. The problem thus remains that none of the bands in the double-difference spectra can easily be assigned to the stoichiometric deprotonation of any single residue. Outside the 1600−1700 cm^{-1} spectral region discussed above, there are only a few discernible bands in the double-difference spectrum, and these generally give rise only to small peaks. It is questionable whether any of them are large enough, e.g., relative to the 1761 cm^{-1} positive band which arises from a single carbonyl stretch vibration, to represent the full deprotonation of any single group.

An alternative to stoichiometric proton release from a single group is that the proton donation role is shared among a number of residues. Time-resolved spectra of the E204Q

mutant, which like R82A is deficient in early proton release (*31*), lack the continuum absorbance changes seen in wild-type bR (*36*). The presence of this continuum absorbance in the wild-type bR → M difference spectrum was previously taken as evidence that the proton-release group is a complex, hydrogen-bonded network of ionizable residues and water molecules (*36*).

We have therefore examined the continuum absorbance changes in the R82A mutant, in which the H^+ release is disrupted. While the continuum absorbance changes were completely abolished in E204Q (*36*), that is not the case in R82A, as seen in Figure 4. Certainly, the continuum absorbance change associated kinetically with the M state is missing in R82A. However, at times approaching 1 ms after photolysis, i.e., as N accumulates (see Figure 2), the continuum absorbance changes in the wild-type bR and R82A mutant begin to coincide. Proton release in R82A measured directly at the extracellular surface takes place with a time constant of 0.73 ms and therefore matches perfectly the delayed continuum absorbance change (*64*). Since little or no N accumulates in the photocycle of E204Q (*36*), it is not clear whether similar continuum absorbance changes are present in its N state.

CONCLUSIONS

Our observation of the loss of the transient continuum absorbance decrease associated with the M state in the R82A mutant supports the previous conclusion that the H^+-release group of bR is not a single residue or water molecule but, instead, involves the participation of several groups that form a hydrogen-bonded network (*36*). On the basis of mutational studies, these should include Arg-82, Glu204, and Glu194, as well as one or more water molcules (*30*, *31*, *33*, *35*, *42*). In unphotolyzed bR, the proton released in M would then be in a rapid equilibrium among various sites in the hydrogen-bonded network. Partial deprotonation signals from each participating functional group would appear in the FT-IR difference spectrum of M according to the change in fractional ionization state of each residue. Thus, the IR difference band intensities would be smaller than expected for the stoichiometric deprotonation of any single group.

Previous models have considered Arg-82 an effector but not an active participant in proton release (*30*, *42*). However, the spectral differences between wild type and R82A (Figure 1) do not rule out ionization changes of Arg-82 between unphotolyzed bR and M. On the contrary, the most straightforward interpretation of the sizable bands observed near 1545 and 1640 cm^{-1} in double-difference spectra of the wild type and R82A (Figure 1C), as well as in double-difference spectra of ^{14}N- and ^{15}N-ψ-Arg-82 bR samples (Figure 7), is that these positive bands correspond to C−N stretch vibrations of Arg-82 in the M state. The unusally low frequencies of these C−N stretch bands could indicate that they originate from a deprotonated arginine, but other types of perturbation on this residue can also be hypothesized to give rise to such frequencies. Further model compound studies will therefore be required to interpret these results more definitively.

The hypothesis that Arg-82 itself contributes to the H^+-release group is widely considered to have been disproved by the observation of submillisecond light-induced H^+ release under nearly physiological conditions in several arginine-82 mutants, e.g., R82Q (*30*). These earlier results certainly demonstrated that Arg-82 deprotonation is not an obligatory component of the fast H^+-release step. However, they do not necessarily rule out the possible participation of Arg-82 in an complex H^+-release group, in which the fractional deprotonation of each residue can easily be shifted as a result of mutation. A more complete clarification of the role of Arg-82 in H^+ release will require careful modeling of both the frequency and IR intensity of the ∼1640 and ∼1545 cm^{-1} vibrations that appear to originate from this residue in the M state.

ACKNOWLEDGMENT

We are grateful to Robert R. Birge, whose NIH grant supported K. Wise and whose encouragement and critical advice was of great help in all phases of this work. Support for specialized instrumentation came from the W. M. Keck Foundation. We are also grateful to Richard Krebs for assistance in sample preparation and to Nicolet Instruments and Bruker Instruments for technical assistance.

REFERENCES

1. Henderson, R., and Unwin, P. N. (1975) *Nature 257*, 28−32.
2. Lozier, R. H., Bogomolni, R. A., and Stoeckenius, W. (1975) *Biophys. J. 15*, 955−962.
3. Oesterhelt, D. (1975) *Ciba Found. Symp.*, 147−167.
4. Kayushin, L. P., and Skulachev, V. P. (1974) *FEBS Lett. 39*, 39−42.
5. Mitsuoka, K., Hirai, T., Murata, K., Miyazawa, A., Kidera, A., Kimura, Y., and Fujiyoshi, Y. (1999) *J. Mol. Biol. 286*, 861−882.
6. Takeda, K., Sato, H., Hino, T., Kono, M., Fukuda, K., Sakurai, I., Okada, T., and Kouyama, T. (1998) *J. Mol. Biol. 283*, 463−474.
7. Luecke, H., Richter, H.-T., and Lanyi, J. K. (1998) *Science 280*, 1934−1937.
8. Kimura, Y., Vassylyev, D. G., Miyazawa, A., Kidera, A., Matsushima, M., Mitsuoka, K., Murata, K., Hirai, T., and Fujiyoshi, Y. (1997) *Nature 389*, 206−211.
9. Pebay-Peyroula, E., Rummel, G., Rosenbusch, J. P., and Landau, E. M. (1997) *Science 277*, 1676−1681.
10. Schertler, G. F., Bartunik, H. D., Michel, H., and Oesterhelt, D. (1993) *J. Mol. Biol. 234*, 156−164.
11. Henderson, R., Baldwin, J. M., Ceska, T. A., Zemlin, F., Beckmann, E., and Downing, K. H. (1990) *J. Mol. Biol. 213*, 899−929.
12. Ceska, T. A., and Henderson, R. (1990) *J. Mol. Biol. 213*, 539−560.
13. Henderson, R., Jubb, J. S., and Whytock, S. (1978) *J. Mol. Biol. 123*, 259−274.
14. Luecke, H., Schobert, B., Richter, H.-T., Cartailler, J. P., and Lanyi, J. K. (1999) *Science 286*, 255−261.
15. Bayley, H., Huang, K.-S., Radhakrishnan, R., Ross, A. H., Takagaki, Y., and Khorana, H. G. (1981) *Proc. Natl. Acad. Sci. U.S.A. 78*, 2225−2229.
16. Braiman, M. S., and Mathies, R. A. (1980) *Biochemistry 19*, 5421−5428.
17. Braiman, M. S., Ahl, P. L., and Rothschild, K. J. (1987) *Proc. Natl. Acad. Sci. U.S.A. 84*, 5221−5225.
18. Rothschild, K. J. (1992) *J. Bioenerg. Biomembr. 24*, 147−167.
19. Gerwert, K., and Hess, B. (1988) *Prog. Clin. Biol. Res. 273*, 321−326.
20. Braiman, M. S., Mogi, T., Marti, T., Stern, L. J., Khorana, H. G., and Rothschild, K. J. (1988) *Biochemistry 27*, 8516−8520.
21. Rothschild, K. J., and Marrero, H. (1982) *Proc. Natl. Acad. Sci. U.S.A. 79*, 4045−4049.

22. Maeda, A., Sasaki, J., Shichida, Y., Yoshizawa, T., Chang, M., Ni, B., Needleman, R., and Lanyi, J. K. (1992) *Biochemistry 31*, 4684−4690.
23. Bousché, O., Braiman, M. S., He, Y.-W., Marti, T., Khorana, H. G., and Rothschild, K. (1991) *J. Biol. Chem. 266*, 11063−11067.
24. Kandori, H., Yamazaki, Y., Hatanaka, M., Needleman, R., Brown, L. S., Richter, H.-T., Lanyi, J. K., and Maeda, A. (1997) *Biochemistry 36*, 5134−5141.
25. Heberle, J., and Dencher, N. A. (1992) *Proc. Natl. Acad. Sci. U.S.A. 89*, 5996−6000.
26. Alexiev, U., Mollaaghababa, R., Scherrer, P., Khorana, H. G., and Heyn, M. P. (1995) *Proc. Natl. Acad. Sci. U.S.A. 92*, 372−376.
27. Balashov, S. P., Govindjee, R., Imasheva, E. S., Misra, S., Ebrey, T. G., Feng, Y., Crouch, R. K., and Menick, D. R. (1995) *Biochemistry 34*, 8820−8834.
28. Kono, M., Misra, S., and Ebrey, T. G. (1993) *FEBS Lett. 331*, 31−34.
29. Otto, H., Marti, T., Holz, M., Mogi, T., Stern, L. J., Engel, F., Khorana, H. G., and Heyn, M. P. (1990) *Proc. Natl. Acad. Sci. U.S.A. 87*, 1018−1022.
30. Govindjee, R., Misra, S., Balashov, S. P., Ebrey, T. G., Crouch, R. K., and Menick, D. (1996) *Biophys. J. 71*, 1011−1023.
31. Brown, L. S., Sasaki, J., Kandori, H., Maeda, A., Needleman, R., and Lanyi, J. K. (1995) *J. Biol. Chem. 270*, 27122−27126.
32. Richter, H., Needleman, R., Kandori, H., Maeda, A., and Lanyi, J. (1996) *Biochemistry 35*, 15461−15466.
33. Richter, H.-T., Brown, L. S., Needleman, R., and Lanyi, J. K. (1996) *Biochemistry 35*, 4054−4062.
34. Brown, L. S., Needleman, R., and Lanyi, J. K. (1996) *Biochemistry 35*, 16048−16054.
35. Dioumaev, A. K., Richter, H.-T., Brown, L. S., Tanio, M., Tuzi, S., Saito, H., Kimura, Y., Needleman, R., and Lanyi, J. K. (1998) *Biochemistry 37*, 2496−2506.
36. Rammelsberg, R., Huhn, G., Lübben, M., and Gerwert, K. (1998) *Biochemistry 37*, 5001−5009.
37. Brown, L. S., Váró, G., Hatanaka, M., Sasaki, J., Kandori, H., Maeda, A., Friedman, N., Sheves, M., Needleman, R., and Lanyi, J. K. (1995) *Biochemistry 34*, 12903−12911.
38. Grigorieff, N., Ceska, T. A., Downing, K. H., Baldwin, J. M., and Henderson, R. (1996) *J. Mol. Biol. 259*, 393−421.
39. Scharnagl, C., and Fischer, S. F. (1996) *Chem. Phys. 212*, 231−246.
40. Lin, G. C., El-Sayed, M. A., Marti, T., Stern, L. J., Mogi, T., and Khorana, H. G. (1991) *Biophys. J. 60*, 172−178.
41. Subramaniam, S., Marti, T., and Khorana, H. G. (1990) *Proc. Natl. Acad. Sci. U.S.A. 87*, 1013−1017.
42. Balashov, S. P., Govindjee, R., Kono, M., Imasheva, E. S., Lukashev, E., Ebrey, T. G., Crouch, R. K., Menick, D. R., and Feng, Y. (1993) *Biochemistry 32*, 10331−10343.
43. Zimányi, L., Váró, G., Chang, M., Ni, B., Needleman, R., and Lanyi, J. K. (1992) *Biochemistry 31*, 8535−8543.
44. Petkova, A. T., Hu, J. G., Bizounok, M., Simpson, M., Griffin, R. G., and Herzfeld, J. (1999) *Biochemistry 38*, 1562−1572.
45. Hatanaka, M., Sasaki, J., Kandori, H., Ebrey, T. G., Needleman, R., Lanyi, J., and Maeda, A. (1996) *Biochemistry 35*, 6308−6312.
46. Oesterhelt, D., and Stoeckenius, W. (1974) *Methods Enzymol. 31*, 667−678.
47. Birge, R. R., Gillespie, N. B., Izaguirre, E. W., Kusnetzow, A., Lawrence, A. F., Singh, D., Song, Q. W., Schmidt, E., Stuart, J. A., Seetharaman, S., and Wise, K. J. (1999) *J. Phys. Chem. B 103*, 10746−10766.
48. Venyaminov, S., and Kalnin, N. N. (1990) *Biopolymers 30*, 1243−1257.
49. Doherty, D. G., Shapira, R. H., and Burnett, W. T., Jr. (1957) *J. Am. Chem. Soc. 79*, 5667−5671.
50. Renthal, R., Chung, Y. J., Escamilla, R., Brown, L. S., and Lanyi, J. K. (1997) *Biophys. J. 73*, 2711−2717.
51. Braiman, M. S., Bousché, O., and Rothschild, K. J. (1991) *Proc. Natl. Acad. Sci. U.S.A. 88*, 2388−2392.
52. Rödig, C., and Siebert, F. (1999) *Appl. Spectrosc. 53*, 893−901.
53. Hutson, M. S., and Braiman, M. S. (1998) *Appl. Spectrosc. 52*, 974−984.
54. Lin, S. W., Fodor, S. P., Miercke, L. J., Shand, R. F., Betlach, M. C., Stroud, R. M., and Mathies, R. A. (1991) *Photochem. Photobiol. 53*, 341−346.
55. Hessling, B., Souvignier, G., and Gerwert, K. (1993) *Biophys. J. 65*, 1929−1941.
56. Braiman, M. S., Briercheck, D. M., and Kriger, K. M. (1999) *J. Phys. Chem. B 103*, 4744−4750.
57. Trindle, C., Braiman, M. S., and Prager, A.-B. (1999) *Int. J. Quantum Chem. 74*, 291−297.
58. Braiman, M. S., Walter, T. J., and Briercheck, D. M. (1994) *Biochemistry 33*, 1629−1635.
59. Brzezinski, B., Urjasz, H., and Zundel, G. (1996) *Biochem. Biophys. Res. Commun. 219*, 273−276.
60. Tanio, M., Tuzi, S., Yamaguchi, S., Kawaminami, R., Naito, A., Needleman, R., Lanyi, J. K., and Saito, H. (1999) *Biophys. J. 77*, 1577−1584.
61. Smith, S. O., Pardoen, J. A., Lugtenburg, J., and Mathies, R. A. (1987) *J. Phys. Chem. 91*, 804−819.
62. Hofrichter, J., Henry, E. R., and Lozier, R. H. (1989) *Biophys. J. 56*, 693−706.
63. Hutson, M. S. (2000) Ph.D. Dissertation, University of Virginia.
64. Alexiev, U., Mollaaghababa, R., Khorana, H. G., and Heyn, M. P. (2000) *J. Biol. Chem. 275*, 13431−13440.

BI000426Q